High-Precision Charm-Quark Mass from Current-Current Correlators in Lattice and Continuum QCD

I. Allison,[1] E. Dalgic,[2] C. T. H. Davies,[3] E. Follana,[4] R. R. Horgan,[5] K. Hornbostel,[6] G. P. Lepage,[7,*] J. Shigemitsu,[4] H. Trottier,[2] and R. M. Woloshyn[1]
(HPQCD Collaboration)

K. G. Chetyrkin,[8] J. H. Kühn,[8] M. Steinhauser,[8] and C. Sturm[9]

[1]TRIUMF, 4004 Wesbrook Mall, Vancouver, BC, V6T 2A3, Canada
[2]Physics Department, Simon Fraser University, Vancouver, British Columbia, Canada
[3]Department of Physics and Astronomy, University of Glasgow, Glasgow G12 8QQ, UK
[4]Physics Department, The Ohio State University, Columbus, Ohio 43210, USA
[5] Department of Applied Mathematics and Theoretical Physics, Cambridge University, Wilberforce Road, Cambridge CB3 0WA, UK
[6]Southern Methodist University, Dallas, Texas 75275, USA
[7]Laboratory for Elementary-Particle Physics, Cornell University, Ithaca, NY 14853, USA
[8]Institut für Theoretische Teilchenphysik, Universität Karlsruhe, D-76128 Karlsruhe, Germany
[9]Physics Department, Brookhaven National Laboratory, Upton, New York 11973, U.S.A.

(Dated: April 24, 2008)

We use lattice QCD simulations, with MILC configurations and HISQ c-quark propagators, to make very precise determinations of moments of charm-quark pseudoscalar, vector and axial-vector correlators. These moments are combined with new four-loop results from continuum perturbation theory to obtain several new determinations of the $\overline{\mathrm{MS}}$ mass of the charm quark. We find $m_c(3\,\mathrm{GeV}) = 0.984\,(16)\,\mathrm{GeV}$, or, equivalently, $m_c(m_c) = 1.266\,(14)\,\mathrm{GeV}$. This agrees well with results from continuum analyses of the vector correlator using experimental data for e^+e^- annihilation (instead of using lattice QCD simulations). These lattice and continuum results are the most accurate determinations to date of this mass. We also obtain a new result for the QCD coupling: $\alpha_{\overline{\mathrm{MS}}}^{(n_f=4)}(3\,\mathrm{GeV}) = 0.230\,(18)$, or, equivalently, $\alpha_{\overline{\mathrm{MS}}}^{(n_f=5)}(M_Z) = 0.113\,(4)$.

PACS numbers: 11.15.Ha,12.38.Aw,12.38.Gc

I. INTRODUCTION

Precise values for the charm quark's mass m_c are important for high-precision tests of the Standard Model. Some of the most accurate determinations currently come from zero-momentum moments of current-current correlators built from the c quark's electromagnetic current (see, for example, [1, 2]). Low moments are perturbative and have long been known through three-loop order [3–5]. New techniques have recently extended these results to much higher moments [6, 7] and, in some cases, to four-loop order [8, 9]. These moments can be estimated nonperturbatively, using dispersion relations, from experimental data for the electron-positron annihilation cross section, $\sigma(e^+e^- \to \gamma^* \to X)$. The c quark's mass is extracted by comparing the perturbative and experimental determinations.

In this paper we show how to compute such moments directly using accurately tuned, highly realistic numerical simulations of QCD in the lattice approximation [10]. As we will show, the correlator moments obtained nonperturbatively from such simulations can be used in place of data from e^+e^- annihilation to obtain new, few-percent accurate determinations of the c quark's mass. With lattice QCD, it is also possible to replace the electromagnetic current in the correlator by the pseudoscalar operator $m_c\overline{\psi}\gamma_5\psi$, thereby providing a completely new set of mass determinations and an important cross check on the entire methodology. In fact our most accurate results come from the pseudoscalar correlators.

In Section II we describe how to compute pseudoscalar correlators and their moments using lattice QCD. We discuss techniques for reducing lattice artifacts in Section III, and present new determinations of $m_c(\mu)$ from our lattice "data" in Section IV. Here we also present a new determination of the QCD coupling. In Section V we extend our analysis to include vector and axial-vector correlators. We summarize our main results in Section VI. In the Appendix we review the continuum perturbation theory needed for this analysis, including new four-loop results for the pseudoscalar case.

II. LATTICE QCD AND PSEUDOSCALAR CORRELATORS

Few-percent accurate QCD simulations have only become possible in the last few years (see, for example, [11, 12]), and accurate simulations of relativistic

*Electronic address: g.p.lepage@cornell.edu

TABLE I: Parameters for the QCD simulations used in this paper. The inverse lattice spacing a^{-1} is in units of GeV; L and T are the spatial and temporal size of the lattices used. The u and d masses are set equal to $m_{u/d}$. The configurations used here were generated by the MILC collaboration [15]. $N_{\rm cfg}$ is the number of configurations used in each case; we used multiple time origins and, in some cases, random wall sources to render statistical errors negligible.

a^{-1}	$am_{0u/d}$	am_{0s}	am_{0c}	L/a	T/a	$N_{\rm cfg}$
1.31	0.013	0.066	0.850	16	48	631
1.60	0.014	0.055	0.660	20	64	595
2.26	0.007	0.037	0.430	28	96	566

c quarks only in the past year — with the new Highly Improved Staggered Quark (HISQ) discretization of the quark action [13, 14], which we use here. A lattice QCD simulation proceeds in two steps. First the QCD parameters — the bare coupling constant and bare quark masses in the Lagrangian — must be tuned. Then the tuned simulation is used to compute vacuum matrix elements of various quantum operators from which physics is extracted. An obvious approach to the tuning is to choose a lattice spacing a, and then tune each of the QCD parameters so that the simulation reproduces the experimental value for a corresponding physical quantity that is well measured. It is more efficient, however, to first choose a value for the bare coupling and then adjust the lattice spacing and bare masses to give physical results.

In the simulations used here, we set the lattice spacing to reproduce the correct $\Upsilon' - \Upsilon$ meson mass difference in the simulations, while we tuned the u/d, s, c and b masses to give correct values for m_π^2, $2m_K^2 - m_\pi^2$, m_{η_c}, and m_Υ, respectively. (For efficiency we set $m_u = m_d$; this leads to negligible errors in the analysis presented here.) The important parameters for the particular simulations used in this paper are listed in Table I; further details can be found in [11, 14]. Once these parameters are set, there are no further physics parameters, and the simulation will accurately reproduce QCD physics for momenta much smaller than the ultraviolet (UV) cutoff ($\Lambda \sim \pi/a$). We have tested these simulations extensively (see, for example, [11, 12]) and, in particular, we have done very precise tests for the charm-quark physics most relevant to this work. These demonstrate, for example, that our simulations reproduce the low-lying spectrum, including spin structure, of both charmonium and heavy-light mesons (D and D_s) to within our simulation uncertainties (a few percent or less) [13, 14].

Given a tuned simulation, it is straightforward to calculate correlators of the sort used to determine m_c. The simplest of these is for the c quark's pseudoscalar density, $j_5 \equiv \overline{\psi}_c \gamma_5 \psi_c$:

$$G(t) \equiv a^6 \sum_{\mathbf{x}} (am_{0c})^2 \langle 0 | j_5(\mathbf{x}, t) j_5(0,0) | 0 \rangle \tag{1}$$

where m_{0c} is the c quark's bare mass (in the lattice Lagrangian). Here time t is euclidean, and the sum over spatial position $\mathbf{x}$ sets the total three momentum to zero. Note that $G(t) = G(T-t) = G(T+t)$ where T is the temporal length of the lattice.

We include two factors of am_{0c} in the definition of $G(t)$ so that $G(t)$ becomes independent of the UV cutoff as $a \to 0$. Consequently the lattice and continuum $G(t)$s become equal in this limit. Moments G_n are trivially computed:

$$G_n \equiv \sum_t (t/a)^n G(t), \tag{2}$$

where, on our periodic lattice [16],

$$t/a \in \{0, 1, 2 \ldots T/2a-1, 0, -T/2a+1 \ldots -2, -1\}. \tag{3}$$

The cutoff independence of $G(t)$ implies that

$$G_n = \frac{g_n(\alpha_{\overline{\rm MS}}(\mu), \mu/m_c)}{(am_c(\mu))^{n-4}} \tag{4}$$

for $n \geq 4$, where $m_c(\mu)$ is the $\overline{\rm MS}$ mass at scale μ and g_n is dimensionless. The c mass can be determined from moments with $n \geq 6$ given G_n from lattice simulations and g_n from perturbation theory (see Appendix). This assumes that perturbation theory is applicable, which should be the case for small enough n.

Note that here and elsewhere in this paper we omit annihilation contributions from $c\bar{c} \to$ gluons $\to c\bar{c}$. This is allowed provided the same contributions are omitted from perturbation theory, which we do. Annihilation contributions to the nonperturbative part of our analysis would be negligible in any case (for example, they shift the η_c mass by approximately 2.4 MeV, which is less than 0.1% [13]).

III. REDUCED MOMENTS

The two biggest challenges for lattice QCD in producing these moments lie in controlling: 1) $\mathcal{O}((am_c)^n)$ errors caused by the lattice approximation; and 2) tuning errors in the QCD parameters, and especially in the lattice spacing and the c quark's bare mass. Each of these potential sources of error is reduced by replacing G_n by a reduced moment:

$$R_n \equiv \begin{cases} G_4/G_4^{(0)} & \text{for } n = 4, \\ \dfrac{am_{\eta_c}}{2am_{0c}} \left(G_n/G_n^{(0)}\right)^{1/(n-4)} & \text{for } n \geq 6, \end{cases} \tag{5}$$

where $G_n^{(0)}$ is the $n^{\rm th}$ moment of the correlator to lowest order in lattice QCD perturbation theory, am_{η_c} is the

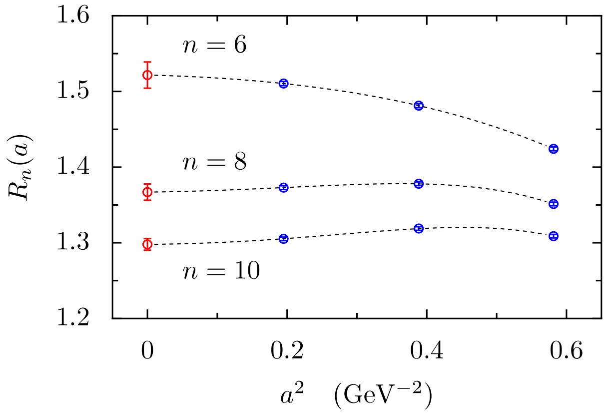

FIG. 1: Reduced moments R_n from lattice simulations with different lattice spacings a. The dashed lines show the functions used to fit the lattice results. These extrapolation functions were used to obtain the $a = 0$ results shown in the plot.

η_c meson mass (in lattice units) from the simulation, and am_{0c} is the bare lattice c mass (in lattice units) used in the simulation. The reduced moments can again be written in terms of continuum quantities:

$$R_n \equiv \begin{cases} r_4(\alpha_{\overline{\mathrm{MS}}}, \mu/m_c) & \text{for } n = 4, \\ \dfrac{r_n(\alpha_{\overline{\mathrm{MS}}}, \mu/m_c)}{2m_c(\mu)/m_{\eta_c}} & \text{for } n \geq 6, \end{cases} \tag{6}$$

where r_n is obtained from g_n (Eq. (4)) and its value, $g_n^{(0)}$, in lowest-order continuum perturbation theory:

$$r_n = \begin{cases} g_4/g_4^{(0)} & \text{for } n = 4, \\ \left(g_n/g_n^{(0)}\right)^{1/(n-4)} & \text{for } n \geq 6. \end{cases} \tag{7}$$

The c mass is obtained from Eq. (6) with $n \geq 6$ using the nonperturbative lattice QCD (LQCD) value for R_n, the perturbative QCD (PQCD) estimate for r_n, and the experimental value for m_{η_c}, 2.980 GeV:

$$m_c(\mu) = \frac{m_{\eta_c}^{\mathrm{exp}}}{2} \, \frac{r_n^{\mathrm{PQCD}}}{R_n^{\mathrm{LQCD}}}. \tag{8}$$

The $G_n^{(0)}$ factor in R_n removes the lattice spacing a from the reduced moment, and cancels all tree-level $\mathcal{O}(a^n)$ errors, thereby reducing finite-a errors overall by about a factor of three [17]. The am_{η_c} factor reduces R_n's sensitivity to slight mistunings of the c quark's bare mass, again by a factor of three. The sensitivity to m_{0c} is reduced because m_c now enters in the ratio m_c/m_{η_c}, so small errors in the simulation parameter m_{0c} are mostly cancelled by corresponding shifts in the simulation value for m_{η_c} [18].

Our simulation results for $R_n(a)$ are listed for different moments n and lattice spacings a in Table II. The uncertainties quoted for each of these values come from two sources. First, for sake of efficiency, we used u/d sea-quark masses that were about 4–5 times too large in

TABLE II: Simulation results for $R_n(a)$ for different lattice spacings a and moments n. The inverse lattice spacing is in GeV. Extrapolations to $a = 0$ are given for each n, together with the corresponding value (in GeV) for $m_c(\mu)$ when $\mu = 3$ GeV.

a^{-1}	1.31	1.60	2.26	$R_n(a=0)$	$m_c(\mu)$
R_4	1.163(1)	1.187(1)	1.223(1)	1.248(25)	–
R_6	1.424(3)	1.481(3)	1.510(3)	1.522(17)	0.990(16)
R_8	1.351(2)	1.378(2)	1.373(2)	1.367(11)	0.980(16)
R_{10}	1.309(2)	1.319(2)	1.305(2)	1.298(8)	0.979(19)
R_{12}	1.274(2)	1.276(2)	1.262(2)	1.256(6)	0.978(23)
R_{14}	1.245(2)	1.244(2)	1.231(2)	1.226(5)	0.978(28)
R_{16}	1.221(2)	1.219(2)	1.207(2)	1.202(4)	0.979(33)
R_{18}	1.201(2)	1.199(2)	1.187(2)	1.183(4)	0.980(39)

our simulations ($m_{u/d}/m_s \approx 0.2$). Simulations with sea masses that were half and twice this value shift our results by less than our 0.2% simulation errors [19]. This error in the moments can also be analyzed using perturbation theory. It implies a fractional error of order $\alpha_s^2(\mu)(m_{u/d}/m_c)^2$, which is much smaller than 0.1%—much too small to justify the effort of extrapolating in the sea masses.

A related concern is the contribution from c-quark vacuum polarization, which we omit from the simulation. The importance of c-quark loops in radiative corrections to the moments can be estimated using perturbation theory. We find that the c-loops add 0.7% to R_4 but less than 0.1% to R_6 and still less for higher moments [20]. We have corrected our R_4 values to account for c loops, and we include an uncertainty of 0.1% in our other reduced moments to allow for any residual uncertainty due to sea-quark masses or the absence of c quarks in the sea.

The second major source of uncertainty, significant for $n \geq 6$ only, comes from residual errors due to mistuning of m_{0c} in the simulation. This results in relative errors of order 0.2%, and an overall tuning error of order 0.5% [21]. We include the former in the errors reported in the Table II for $R_n(a)$, but include the latter only in our final results (since it affects all $R_n(a)$s by the same amount). Other sources of uncertainty in the R_n, like statistics, are negligible compared to these errors.

The reduced moments from the simulation are, as expected, only weakly dependent (few percent) upon the lattice spacing for the lattice spacings we use. To correct for this variation, we extrapolate each moment to $a = 0$ by fitting the simulation values to a function of the form

$$\begin{aligned} R_n(a) = R_n(0)\,(1 &+ c_0(ap_{\mathrm{av}})^2\alpha_s + c_1(am_c)^2(ap_{\mathrm{av}})^2\alpha_s \\ &+ c_2(am_c)^4\alpha_s + c_3(am_c)^6\alpha_s \\ &+ c_4(am_c)^8\alpha_s + \cdots) \end{aligned} \tag{9}$$

where $p_{\mathrm{av}} \approx 7m_c/n$ is the typical three momentum carried by the c quark in the lowest-order perturbation theory diagram for R_n [22]. The extrapolated results depend only weakly on the exact functional form used here provided reasonable Bayesian priors are used for the coefficients c_i. We use the same Gaussian prior, centered at zero with width σ_c, for all of the c_i and all values of n; we tune σ_c to roughly twice the optimal value indicated by the empirical Bayes procedure described in [23]. (This tuning gives $\sigma_c = 1/6$.) This is quite conservative, and leads to uncertainties in our final extrapolated results, $R_n(a=0)$ (see Table II), that are of order the amount of the extrapolation from the finest lattice spacing to $a=0$. Our extrapolations for the $n=6,8,10$ moments are shown in Fig. 1.

IV. EXTRACTING $m_c(\mu)$

To convert the extrapolated reduced moments into c masses, we require perturbative expansions for the r_n in Eq. (8). These are easily computed from the expansions for g_n [3–9] using Eq. (7); details can be found in the Appendix. The perturbative expansions have the form

$$r_n = 1 + r_{n,1}\alpha_{\overline{\rm MS}}(\mu) + r_{n,2}\alpha^2_{\overline{\rm MS}} + r_{n,3}\alpha^3_{\overline{\rm MS}} + \ldots \tag{10}$$

where we set the renormalization scale μ to 3 GeV [24]. The full third-order coefficients for the $n=4,6$ moments were computed for this analysis and are presented in the Appendix. The third-order coefficients for moments with $n \geq 8$ are only partially complete: our analysis includes all μ-dependent terms (that is, $\log^n(\mu/m_c)$ terms), but the constant parts have not yet been computed. Consequently we take the truncation uncertainty in r_n to be of order [25]

$$\sigma_{r_n} = \begin{cases} r_n^{\max}\alpha^4_{\overline{\rm MS}}(\mu) & \text{for } n = 4,6, \\ r_n^{\max}\alpha^3_{\overline{\rm MS}}(\mu) & \text{for } n \geq 8, \end{cases} \tag{11}$$

where

$$r_n^{\max} = \max\left(|r_{n,1}|, |r_{n,2}|, |r_{n,3}|\right). \tag{12}$$

In this paper we use $\alpha_{\overline{\rm MS}}(3\,\text{GeV}) = 0.252\,(10)$ for the ($n_f = 4$) coupling constant. We derived this from the current Particle Data Group average for the $n_f = 5$ coupling at $\mu = M_Z$, which is 0.1176 (20) [26].

Note that coefficients in the r_n expansion, Eq. (10), depend upon $m_c(\mu)$ through scale-dependent logarithms, $\log^n(\mu/m_c(\mu))$. Consequently Eq. (8) is an implicit equation for $m_c(\mu)$, since the mass appears on both sides of the equation. The $m_c(\mu)$-dependence on the right-hand side, however, is suppressed by $\alpha_{\overline{\rm MS}}(\mu)$, and therefore the equation is easily solved numerically.

Our final results for the c-quark's mass, $m_c(\mu)$ at $\mu = 3$ GeV in the $\overline{\rm MS}$ scheme, are listed in Table II, and plotted in the upper-left panel of Figure 2. As is clear from the figure, all moments agree on the mass although the higher moments may be less trustworthy (see [2]).

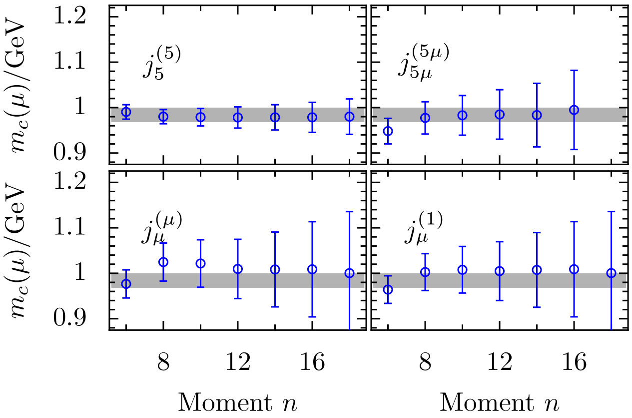

FIG. 2: $m_c(\mu = 3\,\text{GeV})$ from different moments of correlators built from four different lattice operators. The gray band is our final result for the mass, 0.984 (16) GeV, which comes from the first three moments of the pseudoscalar correlator (upper-left panel).

We obtain our final result from the first three moments ($n = 6,8,10$), which average to give:

$$m_c(3\,\text{GeV}) = 0.984\,(16)\,\text{GeV} \tag{13}$$

Evolving down to scale $\mu = m_c(\mu)$ using fourth-order evolution [27–30], this is equivalent to [31]

$$m_c(m_c) = 1.266\,(14)\,\text{GeV}. \tag{14}$$

The leading sources of uncertainty in $m_c(\mu)$ are listed in Table III for each of the four lowest moments. Most of the systematic changes with n in these uncertainties are due to the fact that the moments become increasingly infrared as n increases. Consequently, we are not surprised to see uncertainties related to the convergence of perturbation theory grow as n grows, while uncertainties due to the finite lattice spacing a decrease. Similarly nonperturbative effects in the continuum part of our analysis are expected to be negligible for the lower moments ($n \leq 10$ at least [2]), but could become important for larger n as confinement turns on.

To test for nonperturbative effects, we examined the leading gluon-condensate contribution to our analysis [2, 32, 33]. We did not correct the central values of our masses for condensate contributions because the condensate's size is not well known; but we did add a contribution to the uncertainty for each mass that covers the current range of possible condensate contributions [34]. This has negligible effect on the moments with $n \leq 12$ but becomes quite large as n increases.

There are also uncertainties due to the finite spatial volume of our lattices; our lattices were approximately 2.5 fm across. While our simulations showed no measurable volume dependence [19], lattice perturbation theory shows finite-volume sensitivity for the higher (more infrared) moments. This is negligible for lower moments but grows with n. The finite-volume sensitivity is mostly

TABLE III: Sources of uncertainty in the determinations of $m_c(\mu = 3\,\mathrm{GeV})$ from different reduced moments R_n of the pseudoscalar correlator. The uncertainties listed are percentages of the final result 0.984 (16) GeV.

	R_6	R_8	R_{10}	R_{12}
a^2 extrapolation	1.3%	0.9%	0.7%	0.5%
pert'n theory	0.4	0.9	1.3	1.6
$\alpha_{\overline{\mathrm{MS}}}$ uncertainty	0.3	0.6	1.0	1.3
gluon condensate	0.3	0.0	0.3	0.7
statistical errors	0.0	0.0	0.0	0.0
relative scale errors	0.4	0.4	0.3	0.3
overall scale errors	0.6	0.6	0.7	0.7
sea quarks	0.2	0.2	0.1	0.1
finite volume	0.1	0.1	0.3	0.4
Total	1.6%	1.6%	2.0%	2.4%

an artifact of perturbation theory; confinement significantly reduces finite-volume effects. Consequently we assign a finite-volume error to our perturbative factors that is equal to the entire finite-volume correction in perturbation theory.

One check on the reliability of our analysis comes from the $n = 4$ moment, which is dimensionless. We compared our simulation result for this moment with perturbation theory in order to extract a new value for the QCD coupling. We obtained

$$\alpha_{\overline{\mathrm{MS}}}^{(n_f=4)}(3\,\mathrm{GeV}) = 0.230\,(18) \tag{15}$$

which is equivalent to $\alpha_{\overline{\mathrm{MS}}}^{(n_f=5)}(M_Z) = 0.113(4)$. This agrees well with the Particle Data Group's world average of 0.1176 (20) for the result at $\mu = M_Z$ [26] but is far from being the most accurate determination from either the lattice or the continuum. The bulk of the uncertainty in our new result for the coupling constant comes from uncertainties in the a^2 extrapolation. Our coupling is three to four times more sensitive to such effects than are our mass determinations since the coupling is determined from radiative corrections (which are suppressed by a power of α_s).

V. OTHER CORRELATORS

The close agreement between different moments is important evidence that we understand our systematic errors since these enter quite differently in different moments. To further check this we repeated our analysis for three different correlators, which we formed by replacing the pseudoscalar operator $m_{0c}j_5$ with each of the following c-quark currents on the lattice:

TABLE IV: Simulation results for the reduced moments $R_n^{(j)}$, extrapolated to $a = 0$, from correlators of local axial-vector and vector lattice currents, and a point-split lattice vector current. Corresponding values for $m_c(\mu = 3\,\mathrm{GeV})$ (in GeV) are also given.

	$j_{5\mu}^{(5\mu)}$		$j_\mu^{(\mu)}$		$j_\mu^{(1)}$	
n	$R_n^{(j)}$	$m_c(\mu)$	$R_n^{(j)}$	$m_c(\mu)$	$R_n^{(j)}$	$m_c(\mu)$
6	1.243(13)	0.95(3)	1.256(15)	0.98(3)	1.268(15)	0.96(3)
8	1.167(11)	0.98(4)	1.156(13)	1.02(4)	1.174(13)	1.00(4)
10	1.131(10)	0.98(4)	1.127(12)	1.02(5)	1.137(12)	1.01(5)
12	1.107(10)	0.98(5)	1.113(11)	1.01(7)	1.116(11)	1.01(7)
14	1.086(10)	0.99(7)	1.096(11)	1.01(8)	1.097(11)	1.01(8)
16	1.068(9)	0.99(9)	1.079(11)	1.01(11)	1.079(11)	1.01(11)
18			1.063(11)	1.01(14)	1.063(11)	1.01(14)

$$j_\mu^{(1)} \equiv \overline{\psi}_c(x + a\hat{\mu})\gamma_\mu\psi_c(x), \tag{16}$$

$$j_\mu^{(\mu)} \equiv \overline{\psi}_c(x)\gamma_\mu\psi_c(x), \tag{17}$$

$$j_{5\mu}^{(5\mu)} \equiv \overline{\psi}_c(x)\gamma_5\gamma_\mu\psi_c(x). \tag{18}$$

The first two currents are different lattice discretizations of the vector current and were evaluated for space-like μs; and the first of these was evaluated in Coulomb gauge. The third current is a lattice discretization of the axial vector current and was evaluated for time-like μ. The superscript on each j labels the "taste" carried by that operator, using the notation presented in the Appendices of [13]. Taste is a spurious quantum number, analogous to flavor, that is an artifact of staggered-quark lattice discretizations like the HISQ formalism. Taste should not affect physical results and therefore operators carrying different taste here should give identical results in the $a \to 0$ limit. By studying these different currents, we not only test for conventional systematic errors, but also verify that HISQ-specific taste effects are negligible [35].

A complication in our lattice analysis of these vector (or axial-vector) correlators is that none of the currents is conserved (or partially conserved) on the lattice. Consequently, each lattice current is related to its corresponding continuum operator by a renormalization constant:

$$j_{\mathrm{cont}} = Z^{(j)}\,j + \mathcal{O}(a^2) \tag{19}$$
$$Z^{(j)} \equiv Z^{(j)}(\alpha_{\overline{\mathrm{MS}}}(\pi/a), am_{0c})$$

where j is one of the lattice currents $j_\mu^{(1)}$, $j_\mu^{(\mu)}$, or $j_{5\mu}^{(5\mu)}$, and j_{cont} is the continuum current $j_\mu = \overline{\psi}\gamma_\mu\psi$ for the first two js and $j_{5\mu} = \overline{\psi}\gamma_5\gamma_\mu\psi$ for the last. Consequently moments of the correlators of these lattice currents have the form

$$G_n^{(j)} = \frac{1}{Z^{(j)2}}\,\frac{g_n^{(j_{\mathrm{cont}})}(\alpha_{\overline{\mathrm{MS}}}(\mu), \mu/m_c)}{(am_c(\mu))^{n-2}}. \tag{20}$$

where $Z^{(j)^2}G_n^{(j)}$ is the continuum result for $n \geq 4$. To cancel the renormalization factor we redefine the reduced

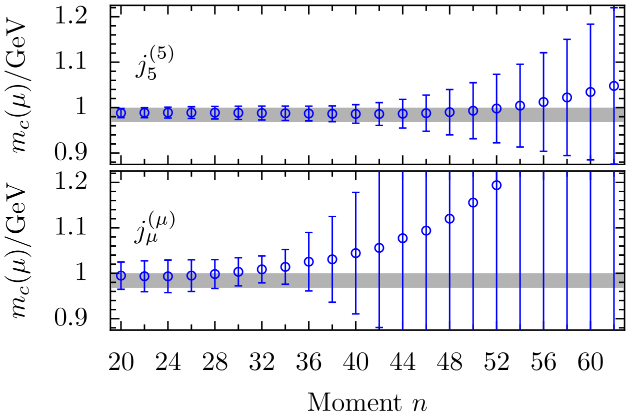

FIG. 3: $m_c(\mu = 3\,\text{GeV})$ from large-n moments of the pseudoscalar and the (local) vector correlators. The gray band is our final result for the mass, 0.984 (16) GeV. The perturbative part of the analysis was evaluated at $\mu = m_c(\mu)$ using formulas from [7], and the results evolved to $\mu = 3\,\text{GeV}$ using fourth-order evolution. Uncertainties due to the gluon condensate are not included (see text).

moments for these correlators to be

$$R_n^{(j)} \equiv \frac{am^{(j)}}{2am_{0c}} \left(\frac{G_n^{(j)}}{G_{n-2}^{(j)}} \frac{G_{n-2}^{(j0)}}{G_n^{(j0)}} \right)^{1/2} \tag{21}$$

$$\equiv \frac{r_n^{(j_{\text{cont}})}(\alpha_{\overline{\text{MS}}}, \mu/m_c)}{2m_c(\mu)/m^{(j)}} \tag{22}$$

where $n \geq 6$, and $m^{(j)}$ is the ψ mass for the vector currents (which couple to the ψ) and the η_c mass for the axial-vector current. Again we divide each moment $G_n^{(j)}$ by its value $G_n^{(j0)}$ in leading-order lattice perturbation theory in order to minimize finite-lattice-spacing errors. And again the perturbative expansion for $r_n^{(j_{\text{cont}})}$ can be obtained from continuum perturbation theory expansions for the $g_n^{(j_{\text{cont}})}$ (see the Appendix).

Our simulation results for $R_n^{(j)}$, extrapolated to lattice spacing $a = 0$, are given in Table IV for different moments n and each of the three currents. Perturbative coefficients for the vector-current $r_n^{(j_{\text{cont}})}$s are discussed in the Appendix; the coefficients for the temporal axial-vector current can be derived from the pseudoscalar coefficients (also in the Appendix) using Ward identities which imply [36]:

$$r_n^{(j_{5\mu})} = \left(r_{n+2}^{n-2} / r_n^{n-4} \right)^{1/2}. \tag{23}$$

By combining perturbative with nonperturbative results, we obtain the values for $m_c(\mu)$, with $\mu = 3\,\text{GeV}$, that are listed in Table IV and plotted in the top-right and bottom panels of Figure 2. Results from all moments agree with each other and with the pseudoscalar result (the gray band in the plots), although here the errors are about twice as large for the smaller moments.

VI. CONCLUSIONS

Our results are by far the most accurate determination of the c-quark mass from lattice QCD [37]. Such precision is possible because the matching between lattice parameters and continuum parameters here relies upon continuum perturbation theory, which is much simpler than lattice QCD perturbation theory. Consequently perturbation theory can be pushed to much higher orders.

The agreement between masses from different moments, and from different correlators — 27 determinations in all — is an important check on systematic errors of all sorts since these enter in very different ways in each calculation. Note that the different reduced moments in our analysis vary in value by as much as 43% (from 1.06 to 1.52), and yet they all agree on the value of m_c to within a few percent once we account for differences in the perturbative parts.

One surprising feature of our results is that even the higher moments give correct values for the quark mass, albeit with larger errors. Nonperturbative effects grow with n but our results show no systematic deviation until very large n, as is evident in Fig. 3 which shows results for $20 \leq n \leq 62$. We have not included potential errors due to the gluon condensate in this figure. The error bars would have been much larger had we done so. For example, they would have been about 5 times larger at $n = 40$ in the pseudoscalar plot (16% rather than 3%). This might suggest that the condensate is smaller than we allowed for — say $\langle \alpha_s G^2/\pi \rangle \leq 0.003\,\text{GeV}^4$ — but we have not analyzed this carefully enough to make a strong statement. The error bars shown in the plots start to grow rapidly just where it becomes clear that perturbation theory is failing (because of large coefficients).

Our lattice result for the mass, $m_c(3\,\text{GeV}) = 0.984\,(16)\,\text{GeV}$, agrees well with the continuum determination, which uses e^+e^- annihilation data and gives 0.986 (13) GeV [2]. This provides further strong evidence that the different systematic errors in each calculation are understood. The lattice analysis will be improved as data becomes available for smaller lattice spacings. Also a very accurate c-quark mass will allow us to make similarly accurate determinations of the s-quark mass [38]. This is because the ratio m_c/m_s can be determined very accurately in lattice simulations where the s and c quarks are analyzed using the same formalism, as here. Finally four-loop perturbation theory for further moments would improve both lattice and continuum determinations.

Acknowledgements

We thank Craig McNeile for useful discussions. We are grateful to the MILC Collaboration for the use of their gluon configurations. The lattice QCD computing was done on UKQCD's QCDOCX cluster and at the Ohio Supercomputer Center. The work was supported by grants from: the Deutsche Forschungsgemeinschaft, SFB-Transregio 9; the Department of Energy (DE-FG02-91-ER40690, DE-AC02-98CH10886(BNL)); the Leverhulme Trust; the Natural Sciences and Engineering Research Council; the National Science Foundation; and the Science and Technology Facilities Council.

k	$\bar{C}_k^{(0)}$	$\bar{C}_k^{(10)}$	$\bar{C}_k^{(11)}$	$\bar{C}_k^{(20)}$	$\bar{C}_k^{(21)}$	$\bar{C}_k^{(22)}$	$\bar{C}_k^{(30)}$	$\bar{C}_k^{(31)}$	$\bar{C}_k^{(32)}$	$\bar{C}_k^{(33)}$
1	1.3333	3.1111	0.0000	0.1154	−6.4815	0.0000	−1.2224	2.5008	13.5031	0.0000
2	0.5333	2.0642	1.0667	7.2362	1.5909	−0.0444	7.0659	−7.5852	0.5505	0.0321
3	0.3048	1.2117	1.2190	5.9992	4.3373	1.1683	—	7.3626	4.2523	−0.0649
4	0.2032	0.7128	1.2190	4.2670	4.8064	2.3873	—	14.7645	11.0345	1.4589
5	0.1478	0.4013	1.1821	2.9149	4.3282	3.4971	—	16.0798	16.6772	4.4685
6	0.1137	0.1944	1.1366	1.9656	3.4173	4.4992	—	14.1098	19.9049	8.7485
7	0.0909	0.0500	1.0912	1.3353	2.2995	5.4104	—	10.7755	20.3500	14.1272
8	0.0749	−0.0545	1.0484	0.9453	1.0837	6.2466	—	7.2863	17.9597	20.4750
1	1.0667	2.5547	2.1333	2.4967	3.3130	−0.0889	−5.6404	4.0669	0.9590	0.0642
2	0.4571	1.1096	1.8286	2.7770	5.1489	1.7524	—	6.7216	6.4916	−0.0974
3	0.2709	0.5194	1.6254	1.6388	4.7207	3.1831	—	7.5736	13.1654	1.9452
4	0.1847	0.2031	1.4776	0.7956	3.6440	4.3713	—	4.9487	17.4612	5.5856
5	0.1364	0.0106	1.3640	0.2781	2.3385	5.3990	—	0.9026	18.7458	10.4981
6	0.1061	−0.1158	1.2730	0.0070	0.9553	6.3121	—	−3.1990	16.9759	16.4817
7	0.0856	−0.2033	1.1982	−0.0860	−0.4423	7.1390	—	−6.5399	12.2613	23.4000
8	0.0709	−0.2660	1.1351	−0.0496	−1.8261	7.8984	—	−8.6310	4.7480	31.1546

TABLE V: Moments of the pseudoscalar (upper 8 lines) and the vector (lower 8 lines) correlators, where currently unknown coefficients are denoted by a dash and set to zero in our analysis. The numbers correspond to QCD with one massive c-quark and three massless (u, d, s) quarks.

Appendix: Continuum perturbation theory

The correlators of two pseudoscalar ($\imath\,\bar{\psi}_c\gamma_5\psi_c$), vector $\bar{\psi}_c\gamma_\mu\psi_c$, and axial-vector $\bar{\psi}_c\gamma_\mu\gamma_5\psi_c$ currents are defined by

$$q^2\Pi^p(q^2) = i\int dx e^{iqx}\langle 0|Tj_5(x)j_5(0)|0\rangle, \qquad (24)$$

$$\begin{aligned}(q_\mu q_\nu - q^2 g_{\mu\nu})\Pi^\delta(q^2) + q_\mu q_\nu \Pi_L^\delta(q^2) &= \Pi_{\mu\nu}^\delta(q)\\ &= i\int dx\, e^{iqx}\langle 0|Tj_\mu^\delta(x)j_\nu^\delta(0)|0\rangle. \qquad (25)\end{aligned}$$

where $\delta = v$ and a for the vector and axial-vector cases, respectively. The polarization functions can be expanded in the variable $z = q^2/(2m_c(\mu))^2$:

$$\bar{\Pi}^\delta(q^2) = \frac{3}{16\pi^2}\sum_{k=-1}^{\infty}\bar{C}_k^\delta z^k. \qquad (26)$$

The polarization function and the c-quark mass $m_c(\mu)$ are renormalized in the $\overline{\mathrm{MS}}$-scheme.

The longitudinal part of the axial-vector current (which is of interest in the present context) and the pseudoscalar correlator are related by the axial Ward-identity[39]:

$$q^\mu q^\nu \Pi_{\mu\nu}^a(q) = (2m)^2 q^2 \Pi^p(q^2) + \text{contact term}. \qquad (27)$$

Comparing different orders in z,

$$\bar{C}_{k+1}^p = \bar{C}_{L,k}^a, \quad \text{for} \quad k \geq -1, \qquad (28)$$

allows us to extract moments of the pseudoscalar correlator from those of the longitudinal part of the axial-vector correlator, and *vice versa*. The contact term contributes only to $k = -2$. The coefficients of the perturbative expansion depend logarithmically on m_c and can be written in the form

$$\begin{aligned}\bar{C}_k &= \bar{C}_k^{(0)} + \frac{\alpha_s(\mu)}{\pi}\left(\bar{C}_k^{(10)} + \bar{C}_k^{(11)} l_{m_c}\right)\\ &+ \left(\frac{\alpha_s(\mu)}{\pi}\right)^2\left(\bar{C}_k^{(20)} + \bar{C}_k^{(21)} l_{m_c} + \bar{C}_k^{(22)} l_{m_c}^2\right)\\ &+ \left(\frac{\alpha_s(\mu)}{\pi}\right)^3\left(\bar{C}_k^{(30)} + \bar{C}_k^{(31)} l_{m_c}\right.\\ &\left. + \bar{C}_k^{(32)} l_{m_c}^2 + \bar{C}_k^{(33)} l_{m_c}^3\right) + \ldots \qquad (29)\end{aligned}$$

where $l_{m_c} \equiv \log(m_c^2(\mu)/\mu^2)$. The coefficients $\bar{C}_k^{(ij)}$ up through $k = 8$ are listed in Table V for both pseudoscalar and vector correlators.

The four-loop coefficients $\bar{C}_1^{(30)}$ and $\bar{C}_2^{(30)}$ for the pseudoscalar correlator are new [40]; and $\bar{C}_1^{(30)}$ for the vector correlator comes from [8, 9]. The order α_s^2 terms up through $k = 8$ are given in [3–5], while results for higher k-values are given in [6, 7]. See also [41] for n_f-dependent four-loop terms, and [7] for the pseudoscalar case. Throughout this paper we take the number of light (massless) active quark flavors to be $n_l = 3$, and the number of heavy (massive) quarks is set to $n_h = 1$. For numerical work, we use $\mu = 3\,\text{GeV}$.

The expansion coefficients $\bar{C}_k$ are related to the coefficients g_n of Eq. (4) by:

$$\frac{g_{2k+2}}{g_{2k+2}^{(0)}} = \frac{\bar{C}_k}{\bar{C}_k^{(0)}}, \tag{30}$$

and the coefficients $r_{n,i}$ in Eq. (10) are obtained through the series expansion of Eq. (7). For the vector correlator the coefficients $r_{n,i}^{(j_\mu)}$ are defined through the series expansions of

$$r_{2k+2}^{(j_\mu)} = \left(\frac{\bar{C}_k^v}{\bar{C}_k^{v,(0)}} \frac{\bar{C}_{k-1}^{v,(0)}}{\bar{C}_{k-1}^v} \right)^{1/2}. \tag{31}$$

[1] J. H. Kuhn and M. Steinhauser, Nucl. Phys. B **619**, 588 (2001) [Erratum-ibid. B **640**, 415 (2002)] [arXiv:hep-ph/0109084].

[2] J. H. Kuhn, M. Steinhauser and C. Sturm, Nucl. Phys. B **778**, 192 (2007) [arXiv:hep-ph/0702103].

[3] K. G. Chetyrkin, J. H. Kuhn and M. Steinhauser, Phys. Lett. B **371**, 93 (1996) [arXiv:hep-ph/9511430].

[4] K. G. Chetyrkin, J. H. Kuhn and M. Steinhauser, Nucl. Phys. B **482**, 213 (1996) [arXiv:hep-ph/9606230].

[5] K. G. Chetyrkin, J. H. Kuhn and M. Steinhauser, Nucl. Phys. B **505**, 40 (1997) [arXiv:hep-ph/9705254].

[6] R. Boughezal, M. Czakon and T. Schutzmeier, Nucl. Phys. Proc. Suppl. **160**, 160 (2006) [arXiv:hep-ph/0607141].

[7] A. Maier, P. Maierhofer and P. Marquard, Nucl. Phys. B **797**, 218 (2008) [arXiv:0711.2636 [hep-ph]].

[8] K. G. Chetyrkin, J. H. Kuhn and C. Sturm, Eur. Phys. J. C **48**, 107 (2006) [arXiv:hep-ph/0604234].

[9] R. Boughezal, M. Czakon and T. Schutzmeier, Phys. Rev. D **74**, 074006 (2006) [arXiv:hep-ph/0605023].

[10] For an earlier exploratory analysis, using less advanced lattice and continuum QCD results, see A. Bochkarev and P. de Forcrand, Nucl. Phys. B **477**, 489 (1996) [arXiv:hep-lat/9505025].

[11] C. T. H. Davies *et al.* [HPQCD Collaboration], Phys. Rev. Lett. **92**, 022001 (2004) [arXiv:hep-lat/0304004].

[12] Q. Mason *et al.* [HPQCD Collaboration], Phys. Rev. Lett. **95**, 052002 (2005) [arXiv:hep-lat/0503005].

[13] E. Follana *et al.* [HPQCD Collaboration], Phys. Rev. D **75**, 054502 (2007) [arXiv:hep-lat/0610092].

[14] E. Follana, C. T. H. Davies, G. P. Lepage and J. Shigemitsu [HPQCD Collaboration], Phys. Rev. Lett. **100**, 062002 (2008) [arXiv:0706.1726 [hep-lat]].

[15] C. Aubin et al, Phys. Rev. D70:094505, 2004.

[16] The value for t/a at the middle of the lattice was set to 0 in order to preserve the symmetry between t and $-t$. This choice causes odd moments to vanish, for example. The value chosen for this point doesn't matter in our analysis because contributions to our moments from this point are negligibly small (because of the exponential falloff in the correlators at large t).

[17] The suppression is by a factor of $\alpha_s(1/a)$, which explains the factor of three.

[18] The ratio m_c/m_{η_c} is independent of m_c up to binding corrections of order $(v_c/c)^2 \approx 1/3$, which is why the suppression is again by roughly a factor of three. See C. T. H. Davies *et al.*, Phys. Rev. Lett. **73**, 2654 (1994) [arXiv:hep-lat/9404012]; A. Gray, I. Allison, C. T. H. Davies, E. Dalgic, G. P. Lepage, J. Shigemitsu and M. Wingate, Phys. Rev. D **72**, 094507 (2005) [arXiv:hep-lat/0507013].

[19] We did additional simulations to test sea-quark mass and spatial volume dependence using $a^{-1} = 1.6\,\text{GeV}$ lattices with: 1) $am_{0u/d} = 0.007$, $L/a = 24$; and 2) $am_{0u/d} = 0.028$, $L/a = 20$.

[20] We computed the contribution from c-quark loops by comparing results from [7] for $n_h = 1$ (with c quarks) with those for $n_h = 0$ (without c quarks). The reduced moments R_n are corrected, to include c quarks, by multiplying them by $r_n(n_h = 1)/r_n(n_h = 0)$.

[21] More specifically these errors come from a 0.5% uncertainty in our ability to measure ratios of lattice spacings, and an overall, correlated 1.5% uncertainty in the measured values of all lattice spacings (see [14]). These errors are all reduced by a factor 1/3 because of our use of reduced moments, as discussed in the text.

[22] We estimate this by inserting a factor of $1/(1+(ap)^2)$ into the Feynman integral for lowest order and calculating the change, ΔG_n, in the moment. The average value of $(ap)^2$ is then approximated by $|\Delta G_n/G_n|$.

[23] G. P. Lepage, B. Clark, C. T. H. Davies, K. Hornbostel, P. B. Mackenzie, C. Morningstar and H. Trottier, Nucl. Phys. Proc. Suppl. **106**, 12 (2002) [arXiv:hep-lat/0110175].

[24] The obvious choice, $\mu = m_c(m_c)$, gives smaller perturbative coefficients for the moments of interest, but $\alpha_{\overline{\text{MS}}}(\mu)$ is substantially larger. Consequently $\mu = 3\,\text{GeV}$ gives smaller errors than $\mu = m_c(m_c)$ despite having somewhat larger expansion coefficients. Differences in the final results are small, however.

[25] This gives a perturbative error that is approximately the same size as the error estimates obtained in [2] by varying the renormalization scale between $\mu = 2$ and $4\,\text{GeV}$. The value for R_6, for example, varies from $+0.5\%$ to -0.4% of the central value as μ is varied over this range; the error estimate from Eq. (11) is $\pm 0.4\%$.

[26] W.-M. Yao *et al.* (Particle Data Group), J. Phys. **G 33**, 1 (2006). We use the Particle Data Group's value of $m_b(m_b) = 4.25\,\text{GeV}$ for the b-quark mass when reducing from $n_f = 5$ to $n_f = 4$.

[27] T. van Ritbergen, J. A. M. Vermaseren and S. A. Larin, Phys. Lett. B **400**, 379 (1997) [arXiv:hep-ph/9701390].

[28] M. Czakon, Nucl. Phys. B **710**, 485 (2005) [arXiv:hep-ph/0411261].

[29] K. G. Chetyrkin, Phys. Lett. B **404**, 161 (1997) [arXiv:hep-ph/9703278].

[30] J. A. M. Vermaseren, S. A. Larin and T. van Ritbergen, Phys. Lett. B **405**, 327 (1997) [arXiv:hep-ph/9703284].

[31] Note that $m_c(m_c) = 1.266\,(14)\,\mathrm{GeV}$ implies that $m_c(1.266\,\mathrm{GeV}) = 1.266\,(20)\,\mathrm{GeV}$. The two have the same central value but different uncertainties. This is because the scale in $m_c(m_c)$ is not fixed but rather varies as $m_c(m_c)$ itself is varied across the interval $1.266 \pm 0.014\,\mathrm{GeV}$.

[32] V. A. Novikov, L. B. Okun, M. A. Shifman, A. I. Vainshtein, M. B. Voloshin and V. I. Zakharov, Phys. Rept. **41**, 1 (1978).

[33] D. J. Broadhurst, P. A. Baikov, V. A. Ilyin, J. Fleischer, O. V. Tarasov and V. A. Smirnov, Phys. Lett. B **329**, 103 (1994) [arXiv:hep-ph/9403274].

[34] We include the gluon condensate by multiplying r_n by a factor of the form $(1+d_n\langle\alpha_s G^2/\pi\rangle/(2m_c)^4))$ where, here, $m_c = m_c(m_c)$ and d_n is computed through leading order in $\alpha_{\overline{\mathrm{MS}}}(m_c)$. We set $\langle\alpha_s G^2/\pi\rangle = 0 \pm 0.012\,\mathrm{GeV}^4$, which covers the range of most current values. For a recent analysis of condensate values see B. L. Ioffe, Prog. Part. Nucl. Phys. **56**, 232 (2006) [arXiv:hep-ph/0502148].

[35] A related problem is that correlators built from these currents are contaminated by contributions from correlators built from opposite-parity operators (see Appendix G of [13]). These lattice artifacts oscillate in sign, like $(-1)^{t/a}$, and so are suppressed by $(am_c/\pi)^{n-2}$ in the n^{th} moment since the sum over t is dominated by $E \approx 0$. This makes them negligible except possibly for $n = 4$; the slightly lower masses we obtain from ratios of $n = 6$ and 4 moments may be due to this effect. Such contamination is absent in the case of the pseudoscalar correlators.

[36] The continuum Ward identity relates the axial vector current to the pseudoscalar density [39], implying that $g_n^{(j_{5\mu})} \propto g_{n+2}$ where the g_ns are defined in equations (20) and (4).

[37] For older analyses that include sea quarks see: A. Dougall, C. M. Maynard and C. McNeile, JHEP **0601**, 171 (2006) [arXiv:hep-lat/0508033]; and M. Nobes and H. Trottier, PoS **LAT2005**, 209 (2006) [arXiv:hep-lat/0509128]. The precision of analyses that do not include sea quarks is hard to quantify because the value of the c-mass depends upon how the lattice spacing and the bare c-mass are tuned, and it is not possible to obtain consistency from different choices. For example, tuning the bare mass to give the correct D_s mass gives very different results from tuning to get the correct $D_s^* - D_s$ mass difference, or the correct η_c or ψ mass. We avoid these problems here by including the full effect of sea quarks. For determinations of the c-mass without sea quarks with further discussion of these issues see: J. Rolf and S. Sint [ALPHA Collaboration], JHEP **0212**, 007 (2002) [arXiv:hep-ph/0209255]; and G. M. de Divitiis, M. Guagnelli, R. Petronzio, N. Tantalo and F. Palombi, Nucl. Phys. B **675**, 309 (2003) [arXiv:hep-lat/0305018].

[38] In preparation.

[39] D. J. Broadhurst, Phys. Lett. B **101**, 423 (1981).

[40] Details of the calculation, as well as analytical results, will be presented in C. Sturm, in preparation.

[41] M. Czakon and T. Schutzmeier, arXiv:0712.2762 [hep-ph].